Water Science and Engineering 2019, 12(3): 196–204

HOSTED BY

ELSEVIER

Available online at www.sciencedirect.com

Water Science and Engineering

journal homepage: http://www.waterjournal.cn

Long-term deformation analysis of Shuibuya concrete face rockfill dam based on response surface method and improved genetic algorithm

Fu-hai Yao [a], Shao-heng Guan [a], He Yang [b,*], Yuan Chen [a], Huan-feng Qiu [c], Gang Ma [a], Qi-wen Liu [c]

[a] *School of Water Resources and Hydropower Engineering, Wuhan University, Wuhan 430072, China*
[b] *School of Civil Engineering and Architecture, Wuhan University, Wuhan 430070, China*
[c] *Guiyang Engineering Corporation Limited, Guiyang 550081, China*

Received 10 January 2019; accepted 12 May 2019
Available online 6 September 2019

Abstract

Due to the size effects of rockfill materials, the settlement difference between numerical simulation and in situ monitoring of rockfill dams is a topic of general concern. The constitutive model parameters obtained from laboratory triaxial tests often underestimate the deformation of high rockfill dams. Therefore, constitutive model parameters obtained by back analysis were used to calculate and predict the long-term deformation of rockfill dams. Instead of using artificial neural networks (ANNs), the response surface method (RSM) was employed to replace the finite element simulation used in the optimization iteration. Only 27 training samples were required for RSM, improving computational efficiency compared with ANN, which required 300 training samples. RSM can be used to describe the relationship between the constitutive model parameters and dam settlements. The inversion results of the Shuibuya concrete face rockfill dam (CFRD) show that the calculated settlements agree with the measured data, indicating the accuracy and efficiency of RSM.

Keywords: Shuibuya rockfill dam; Parameter back analysis; Response surface method; Duncan EB model; Time-dependent deformation

1. Introduction

Evaluation of the current working state and an accurate prediction of the deformation are the keys to ensuring the security and stability of a rockfill dam. Due to the size effect, the constitutive model parameters obtained from the laboratory test of a scaled sample cannot accurately characterize the mechanical properties of prototype rockfill materials. Zhou et al. (2018) applied the rate-dependent breakage theory and breakage-energy scaling law in settlement analysis of the Shuibuya concrete face rockfill dam (CFRD) in China. They found that neglecting the scaling and creep effects of rockfill materials will underestimate the maximum settlement of the dam by 14% and 18%, respectively. Therefore, the back analysis of rockfill constitutive parameters, which is based on the measured deformation of a built dam, has been widely used in engineering practice. Generally, we need to construct an objective function based on the monitored and calculated settlements and transform the parameter back analysis into an optimization problem.

Yeh (1986) classified parameter inversion methods into direct and indirect approaches. The direct ones require a large number of finite element simulations, which consume significant computational power and time (Zhang and He, 2005; Saboya and Byrne, 1993). The indirect approaches, such as artificial neural networks (ANNs), which can circumvent the time-consuming finite element simulations, have been

This work was supported by the National Natural Science Foundation of China (Grant No. 51579193) and the Science and Technology Planning Project of Guizhou Province (Grant No. [2016]1154).
* Corresponding author.
E-mail address: 1019463985@qq.com (He Yang).
Peer review under responsibility of Hohai University.

https://doi.org/10.1016/j.wse.2019.09.004

generally employed. An intelligent back analysis method, based on evolutionary neural networks (NNs) and sequential quadratic programming (SQP), was developed to predict the post-deformation of dams (Zhou et al., 2007, 2010). Li et al. (2004) and Zhou et al. (2011a) employed a genetic algorithm (GA) for the back analysis of rockfill parameters. Chang et al. (2011) proposed a novel migrated particle swarm optimization (MPSO) to search for the creep model parameters of rockfill materials. Zhou et al. (2016c) combined a modified GA with radial basis function neural networks (RBFNNs) to perform the parameter back analysis of a high central earth core rockfill dam. Various kinds of ANNs and optimization algorithms (Ma et al., 2012; Tian et al., 2014; Zhu et al., 2010; Wang et al., 2014b; Dong et al., 2012; Liu et al., 2014; Zhang et al., 2011; Zhou et al., 2011b; Wu et al., 2014; Cao et al., 2012) have been proposed for parameter inversion of rockfill dams. However, lots of finite element simulations are required to prepare enough data for training ANNs. Zheng et al. (2013) proposed a method based on multi-output support vector machines to take place the finite element calculation.

To improve computational efficiency, researchers employed the response surface model for parameter back analysis (Yang et al., 2001, 2012; Gui and Kang, 2005; Su et al., 2009; Ji et al., 2014). Abusam et al. (2001) applied the response surface method (RSM) to the parameter estimation of nonlinear systems. With further improvements, the RSM has been widely used in geotechnical engineering, such as parameter back analysis (He et al., 2012), slope stability analysis (Li et al., 2010), and seepage stability analysis (Hu et al., 2012). Yang et al. (2017) proposed an elastoplastic model based on experimental investigation. Li et al. (2014) developed a polynomial response surface function for the inversion of rockfill constitutive parameters. However, the time-dependent effects on deformation of rockfill materials are not considered. This study performed parameter back analysis of the Shuibuya CFRD based on RSM. A response surface function considering both the Duncan EB model and five-parameter creep model parameters of rockfill materials was proposed.

2. Constitutive model

The determination of mechanical parameters of rockfill materials is crucial to engineering design. Back analysis is a helpful technique for evaluation of rockfill parameters. It considers the deformation measured by interior and exterior settlement monitoring systems, such as the interferometric synthetic aperture radar (Zhou et al., 2016a, 2016b). In this study, the instantaneous deformation was described by the Duncan EB model and the rheological deformation was considered using the creep model (Shen and Zhao, 1998).

2.1. Duncan EB model

In the Duncan EB model, the stress-strain relationship is hyperbolic, and the rockfill modulus is a function of confining pressure and shear stress. The rockfill parameters in the model can be obtained from triaxial tests or typical values of corresponding rockfill materials from literature (Shen and Zhao, 1998; Zhou et al., 2007; Zhang et al., 2008; Chang et al., 2011; Cao et al., 2012). The tangent modulus E_t can be expressed as follows:

$$E_t = KP_a\left(\frac{\sigma_3}{P_a}\right)^n\left(1 - SR_f\right)^2 \tag{1}$$

where K is the tangent modulus coefficient, σ_3 is the minor principal stress, P_a is the atmospheric pressure, and R_f is the failure ratio. The exponent n describes the influence of the confining pressure on the initial modulus. The shear stress level S can be expressed as follows:

$$S = \frac{(1 - \sin\varphi)(\sigma_1 - \sigma_3)}{2c\cos\varphi + 2\sigma_3\sin\varphi} \tag{2}$$

$$\varphi = \varphi_0 - \Delta\varphi \lg\left(\frac{\sigma_3}{P_a}\right) \tag{3}$$

where σ_1 is the maximum principal stress, c is the cohesive force, φ_0 is the internal friction angle when the confining pressure reaches the standard atmospheric pressure, and $\Delta\varphi$ equals the reduction of the friction angle when σ_3 is ten times of P_a.

The bulk modulus B_t is given by

$$B_t = K_b P_a\left(\frac{\sigma_3}{P_a}\right)^m \tag{4}$$

where K_b is the bulk modulus and m is the bulk modulus exponent.

2.2. Creep model of rockfill

Shen and Zhao (1998) proposed a three-parameter creep model with exponential decay. Fully considering the obvious rheological increase of rockfill under high confining pressure and a high stress level, Wang et al. (2014a) proposed the following five-parameter creep model based on the exponential decay Merchant model. Numerical researches indicates that rockfill creep obviously influences the deformation and stress of the concrete-face slab (Lei et al., 2014). The creep strain ($\varepsilon(t)$) at time t can be expressed by the power function as follows:

$$\varepsilon(t) = \varepsilon_f\left(1 - e^{-\alpha t}\right) \tag{5}$$

where α is the decay index of creep deformation with time, and ε_f equals the final creep deformation that contains the final volumetric rheology ε_{vf} and the final shearing rheology ε_{sf}:

$$\varepsilon_{vf} = b\left(\frac{\sigma_3}{p_a}\right)^{m_c} + \beta S \tag{6}$$

$$\varepsilon_{sf} = d\frac{S}{1 - S} \tag{7}$$

where b, m_c, β, and d are creep model parameters obtained from the triaxial test.

It can be seen that there are five parameters in the creep model: α, b, m_c, β, and d. All of them can be calibrated using a series of creep triaxial tests.

3. Response surface method

3.1. Response surface function

For the rockfill deformation, the response surface function expresses the relationship between the deformation of a series of measuring points and the parameters to be studied (Wang et al., 2005; Dou et al., 2007; Guo et al., 2016). According to the Duncan EB model and creep model of rockfill, the response surface function of rockfill is based on a mathematical model. As the parameters of the creep model are much smaller than those of the Duncan EB model, it is more reasonable to use the exponential function $\sum_{j=1}^{M} f_j e^{\bar{y}_j}$, rather than a quadratic function $\sum_{i=1}^{N} f_i \bar{y}_i^2$, to consider the nonlinear effect of the rheological parameters.

$$S_k(\bar{\boldsymbol{x}}) = a + \sum_{i=1}^{N} b_i \bar{x}_i + \sum_{i=1}^{N} c_i \bar{x}_i^2 + \sum_{j=1}^{M} d_j \bar{y}_j + \sum_{j=1}^{M} f_j e^{\bar{y}_j} \tag{8}$$

where $S_k(\bar{\boldsymbol{x}})$ is the deformation of the measuring point k; a, b_i, c_i, d_j, and f_j are the coefficients that need to be determined in the response surface function; and N and M are the numbers of Duncan EB model parameters and creep model parameters to be inverted, respectively. $\bar{\boldsymbol{x}}$ and $\bar{\boldsymbol{y}}$ are the dimensionless parameter vectors of the Duncan EB model and creep model, respectively:

$$\bar{\boldsymbol{x}} = (\overline{K}_1, \overline{n}_1, \overline{K}_{b1}, \overline{m}_1, \overline{K}_2, \overline{n}_2, \overline{K}_{b2}, \overline{m}_2)^T \tag{9}$$

$$\bar{\boldsymbol{y}} = (\overline{\alpha}, \overline{b}, \overline{\beta}, \overline{m}_c, \overline{d})^T \tag{10}$$

$$\overline{K}_1 = \frac{K_1}{K_{10}},\ \overline{n}_1 = \frac{n_1}{n_{10}},\ \overline{K}_{b1} = \frac{K_{b1}}{K_{b10}},\ \overline{m}_1 = \frac{m_1}{m_{10}},\ \overline{K}_2 = \frac{K_2}{K_{20}},\ \overline{n}_2 = \frac{n_2}{n_{20}},$$
$$\overline{K}_{b2} = \frac{K_{b2}}{K_{b20}},\ \overline{m}_2 = \frac{m_2}{m_{20}},\ \overline{\alpha} = \frac{\alpha}{\alpha_0},\ \overline{b} = \frac{b}{b_0},\ \overline{\beta} = \frac{\beta}{\beta_0},\ \overline{m}_c = \frac{m_c}{m_{c0}},\ \overline{d} = \frac{d}{d_0} \tag{11}$$

where K_{10}, n_{10}, K_{b10}, m_{10}, K_{20}, n_{20}, K_{b20}, m_{20}, α_0, b_0, β_0, m_{c0}, and d_0 are the initial values of each parameter; and K_1, n_1, K_{b1}, m_1, K_2, n_2, K_{b2}, m_2, α, b, β, m_c, and d are the scaled initial values (subscript 1 represents the primary rockfill zone and subscript 2 represents the secondary rockfill zone).

3.2. Inversion process based on RSM and improved GA

As is shown in Fig. 1, the basic procedure for inverting the constitutive parameters of the high rockfill dam based on RSM is as follows:

(1) Parameter sensitivity analysis. In order to improve the inversion efficiency, Li et al. (2013) proposed the sensitivity analysis of Duncan EB model parameters based on the orthogonal test method. Through this method, it was found φ_0, K, n, K_b, and m to be largely related with the vertical displacement of the dam, which provided a reference for selecting the sensitive Duncan EB model parameters to be inverted.

(2) Construction of the response surface function. The rockfill deformation mainly includes instantaneous and creep deformations. The response surface function, which includes Duncan EB and creep model parameters, is constructed as shown in Eq. (8).

(3) Finite element calculation. Based on the experimental parameters, a combination of parameters is constructed in Eq. (11). The finite element calculation is performed using the combination of these parameters. As shown in Eq. (12), a set of equations for each measuring point is set up (the subscripts and superscripts are the numbers of the measuring points and equations, respectively).

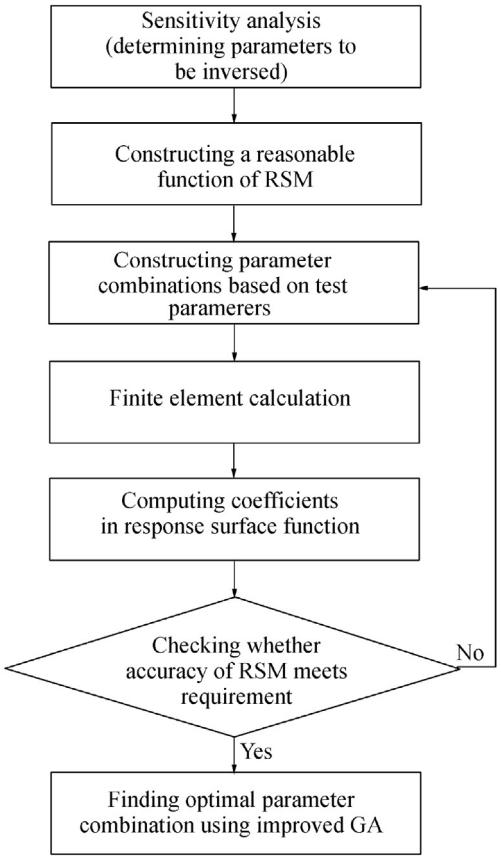

Fig. 1. Flow diagram of back analysis of instantaneous and rheological parameters by RSM.

$$\begin{cases} S_k^1(\bar{\boldsymbol{x}}) = S(\bar{x}_1, \bar{x}_2, \cdots, \bar{x}_N, \bar{y}_1, \bar{y}_2, \cdots, \bar{y}_M) \\ S_k^2(\bar{\boldsymbol{x}}) = S(\bar{x}_1 + \mathrm{d}\bar{x}_1, \bar{x}_2, \cdots, \bar{x}_N, \bar{y}_1, \bar{y}_2, \cdots, \bar{y}_M) \\ S_k^3(\bar{\boldsymbol{x}}) = S(\bar{x}_1 - \mathrm{d}\bar{x}_1, \bar{x}_2, \cdots, \bar{x}_N, \bar{y}_1, \bar{y}_2, \cdots, \bar{y}_M) \\ \vdots \\ S_k^{2(M+N)}(\bar{\boldsymbol{x}}) = S(\bar{x}_1, \bar{x}_2, \cdots, \bar{x}_N, \bar{y}_1, \bar{y}_2, \cdots, \bar{y}_M + \mathrm{d}\bar{y}_M) \\ S_k^{2(M+N)+1}(\bar{\boldsymbol{x}}) = S(\bar{x}_1, \bar{x}_2, \cdots, \bar{x}_N, \bar{y}_1, \bar{y}_2, \cdots, \bar{y}_M - \mathrm{d}\bar{y}_M) \end{cases} \tag{12}$$

(4) Solution of the response surface function for each measuring point. According to Eq. (8), for each measuring point, the number of coefficients required to calculate (Q) and the total number of parameters to invert ($M + N$) satisfy the relationship $Q = 2(M + N) + 1$. The combination of parameters in the form of Eq. (11) has $2(M+N) + 1$ groups, and $2(M+N) + 1$ equations can be formed using the finite element calculation. The number of linear equations is equal to the number of coefficients that need to be determined at each measuring point, so the method can be used to obtain the unique response surface function for each measuring point.

(5) Construction of an objective function to obtain the optimal solution after the response surface function of each measuring point is determined. According to the calculated values of the displacement and measured values of the measuring points, the objective function is a function of the minimum root mean square error (Yeh, 1986). The optimal parameter combination is determined using the improved GA to obtain the optimal solution of the objective function. Thus, the inversion results are obtained.

4. Settlement back analysis

4.1. Parameter sensitivity analysis

The Shuibuya CFRD, with a dam height of 233 m, is located in Hubei Province, China. It was built in 2006. Using the Shuibuya CFRD as an example, the method described above was applied to the inversion of Duncan EB and creep model parameters. Because the two rockfill zones use identical creep parameters, there are only five creep model parameters to be inverted. Duncan EB model parameters K, n, K_b, and m were selected for inversion based on the sensitivity analysis (Hai and Wang, 2005; Sun et al., 2016; Sheng et al., 2012). Because parameters of different zones in the dam vary significantly, as shown in Table 1 and Fig. 2, eight instantaneous parameters of the two rockfill materials should be inverted. In total, there are 13 parameters to be inverted: α, b, β, m_c, d, K_1, n_1, K_{b1}, m_1, K_2, n_2, K_{b2}, and m_2.

4.2. Generation of training samples for response surface function

The three-dimensional (3D) finite element model of the Shuibuya CFRD is shown in Fig. 3, and the situations of the measuring points are shown in Fig. 4. Based on the test

Table 1
Twenty-seven sets of parameter combination for finite element analysis.

Set of parameters	Instantaneous parameter							Rheological parameter					
	K_1	n_1	K_{b1}	m_1	K_2	n_2	K_{b2}	m_2	α	b (10^5)	m_c	β (10^3)	d (10^3)
Experimental	1100	0.35	600	0.10	850	0.25	400	0.05	0.0090	9.80	1.13380	6.40	2.10
1	1100	0.35	600	0.10	850	0.25	400	0.05	0.0090	9.80	1.13380	6.40	2.10
2	1320	0.35	600	0.10	850	0.25	400	0.05	0.0090	9.80	1.13380	6.40	2.10
3	880	0.35	600	0.10	850	0.25	400	0.05	0.0090	9.80	1.13380	6.40	2.10
4	1100	0.42	600	0.10	850	0.25	400	0.05	0.0090	9.80	1.13380	6.40	2.10
5	1100	0.28	600	0.10	850	0.25	400	0.05	0.0090	9.80	1.13380	6.40	2.10
6	1100	0.35	720	0.10	850	0.25	400	0.05	0.0090	9.80	1.13380	6.40	2.10
7	1100	0.35	480	0.10	850	0.25	400	0.05	0.0090	9.80	1.13380	6.40	2.10
8	1100	0.35	600	0.12	850	0.25	400	0.05	0.0090	9.80	1.13380	6.40	2.10
9	1100	0.35	600	0.08	850	0.25	400	0.05	0.0090	9.80	1.13380	6.40	2.10
10	1100	0.35	600	0.10	1020	0.25	400	0.05	0.0090	9.80	1.13380	6.40	2.10
11	1100	0.35	600	0.10	680	0.25	400	0.05	0.0090	9.80	1.13380	6.40	2.10
12	1100	0.35	600	0.10	850	0.30	400	0.05	0.0090	9.80	1.13380	6.40	2.10
13	1100	0.35	600	0.10	850	0.20	400	0.05	0.0090	9.80	1.13380	6.40	2.10
14	1100	0.35	600	0.10	850	0.25	480	0.05	0.0090	9.80	1.13380	6.40	2.10
15	1100	0.35	600	0.10	850	0.25	320	0.05	0.0090	9.80	1.13380	6.40	2.10
16	1100	0.35	600	0.10	850	0.25	400	0.06	0.0090	9.80	1.13380	6.40	2.10
17	1100	0.35	600	0.10	850	0.25	400	0.04	0.0090	9.80	1.13380	6.40	2.10
18	1100	0.35	600	0.10	850	0.25	400	0.05	0.0108	9.80	1.13380	6.40	2.10
19	1100	0.35	600	0.10	850	0.25	400	0.05	0.0072	9.80	1.13380	6.40	2.10
20	1100	0.35	600	0.10	850	0.25	400	0.05	0.0090	11.76	1.13380	6.40	2.10
21	1100	0.35	600	0.10	850	0.25	400	0.05	0.0090	7.84	1.13380	6.40	2.10
22	1100	0.35	600	0.10	850	0.25	400	0.05	0.0090	9.80	1.36056	6.40	2.10
23	1100	0.35	600	0.10	850	0.25	400	0.05	0.0090	9.80	0.90704	6.40	2.10
24	1100	0.35	600	0.10	850	0.25	400	0.05	0.0090	9.80	1.13380	7.68	2.10
25	1100	0.35	600	0.10	850	0.25	400	0.05	0.0090	9.80	1.13380	5.12	2.10
26	1100	0.35	600	0.10	850	0.25	400	0.05	0.0090	9.80	1.13380	6.40	2.52
27	1100	0.35	600	0.10	850	0.25	400	0.05	0.0090	9.80	1.13380	6.40	1.68

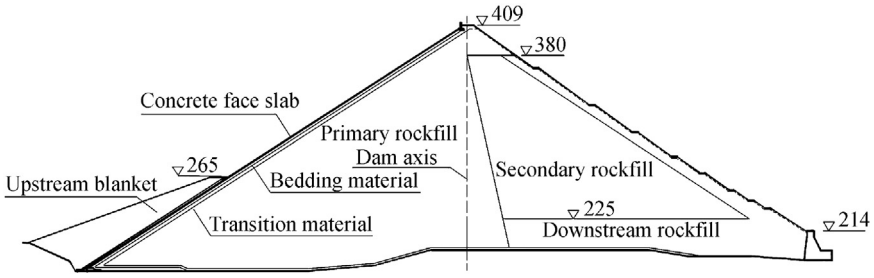

Fig. 2. Schematic diagram of dam zoning of Shuibuya CFRD (units: m).

parameters, 27 sets of parameters were generated, as shown in Table 1. Solving the equations in Eq. (12), the response surface function of each measuring point was obtained.

4.3. Solving response surface function of each measuring point

To reflect the overall deformation of the dam, the completion period, impoundment period, and stable period were selected as three moments to study. The corresponding equation of response surface functions for each measuring point were built at these three moments using Eqs. (11) and (12). Using measuring point 1 as an example, the variables of RSM were obtained by solving Eq. (12), as shown in Table 2. Thus, the response surface function of each measuring point at different moments was confirmed.

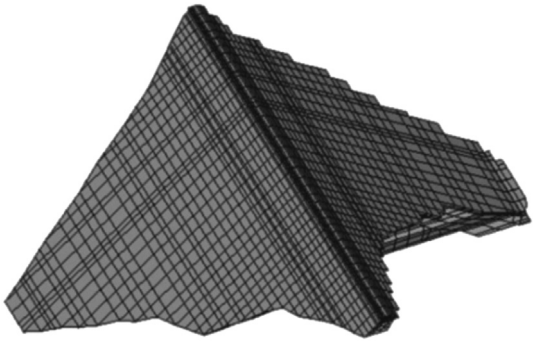

Fig. 3. Finite element model of Shuibuya CFRD.

For the Shuibuya CFRD, the method described above to obtain the RSM only requires 27 sets of training samples, whereas 300 samples are required to invert only seven instantaneous parameters of the Duncan EB model using the NN (Ma et al., 2012). Thus, the RSM has an obvious advantage in computational efficiency.

Regarding calculation accuracy, random sets of parameters were generated and finite element calculation was conducted to verify the prediction precision of the RSM. As shown in Table 3 (three sets of parameters are used as an example), the RSM has a high prediction accuracy, and the largest relative error is about 0.39%, which proves that the RSM has built a relatively accurate mapping relation between the constitutive parameters and the displacement of the measuring points.

To further study the effect of creep model parameters on forecast results, the average relative error of prediction accuracy of the RSM was calculated for the randomly generated calculation parameters of the same set, with and without consideration of the creep deformation of three moments, as shown in Fig. 5. The relative prediction error of the RSM was approximately 18% without considering the creep deformation. However, when the creep model parameter inversion was considered, the relative prediction error of RSM decreased to below 1%, which proves the necessity for consideration of the creep model parameters.

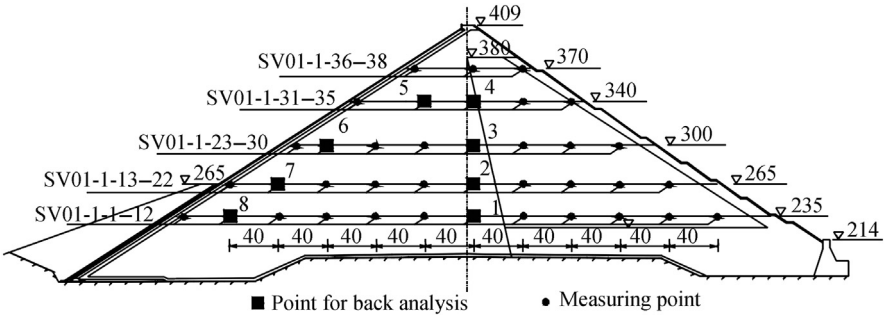

Fig. 4. Schematic diagram of measuring points in (0 + 212 m) section (units: m).

Table 2
Corresponding coefficients of response surface function for measuring point 1 at different moments.

Period	a	b_1	b_2	b_3	b_4	b_5	b_6	b_7	b_8
Completion period	2.5664	0.2965	0.0885	1.8077	0.0760	0.0200	0.0138	0.1495	0.0040
Impoundment period	2.6885	0.2937	0.0877	1.8877	0.0835	0.0295	0.0180	0.1540	0.0045
Stable period	2.6496	0.2895	0.0890	1.8703	0.0820	0.0235	0.0152	0.1507	0.0017
Period	c_1	c_2	c_3	c_4	c_5	c_6	c_7	c_8	d_1
Completion period	0.0850	0.0100	0.5687	0.0025	0.0025	0.0013	0.0350	0.0000	0.0023
Impoundment period	0.0812	0.0087	0.5912	0.0025	0.0000	0.0025	0.0350	0.0000	0.0235
Stable period	0.0800	0.0100	0.5862	0.0025	0.0025	0.0012	0.0337	0.0013	0.0240
Period	d_2	d_3	d_4	d_5	f_1	f_2	f_3	f_4	f_5
Completion period	0.0378	0.0950	0.1001	0.0018	0.0028	0.0009	0.0651	0.0073	0.0009
Impoundment period	0.0410	0.1335	0.1058	0.0013	0.0037	0.0000	0.0862	0.0083	0.0009
Stable period	0.0415	0.1320	0.1086	0.0013	0.0037	0.0000	0.0862	0.0092	0.0009

Table 3
Random verification results of response surface function (example: three sets of parameters).

Period	Number of measuring point	Result of Group A			Result of Group B			Result of Group C		
		Response surface prediction value (m)	Finite element calculation value (m)	Relative error (%)	Response surface prediction value (m)	Finite element calculation value (m)	Relative error (%)	Response surface prediction value (m)	Finite element calculation value (m)	Relative error (%)
Completion period	1	1.0398	1.0403	0.0495	1.6229	1.6229	0.0030	1.7097	1.7099	0.0112
	2	1.0395	1.0407	0.1157	1.6434	1.6476	0.2605	1.7516	1.7584	0.3891
	3	1.0963	1.0974	0.1019	1.7524	1.7281	0.1518	1.8273	1.8311	0.2083
Impoundment period	1	1.1014	1.1022	0.0734	1.7407	1.7410	0.0203	1.9017	1.9017	0.0013
	2	1.1004	1.1016	0.1128	1.7619	1.7665	0.2610	1.9486	1.9548	0.3159
	3	1.1625	1.1640	0.1248	1.8529	1.8558	0.1608	2.0356	2.0389	0.1647
Stable period	1	1.0889	1.0898	0.0782	1.7185	1.7184	0.0064	1.8680	1.8675	0.0288
	2	1.0878	1.0893	0.1328	1.7396	1.7436	0.2303	1.9150	1.9209	0.3096
	3	1.1497	1.1513	0.1343	1.8299	1.8325	0.1440	2.0009	2.0039	0.1477

4.4. Searching for optimal parameter combination

For the objective function construction, the equal-weight method was used to comprehensively consider three characteristic moments: the completion period, the impoundment period, and the stable period.

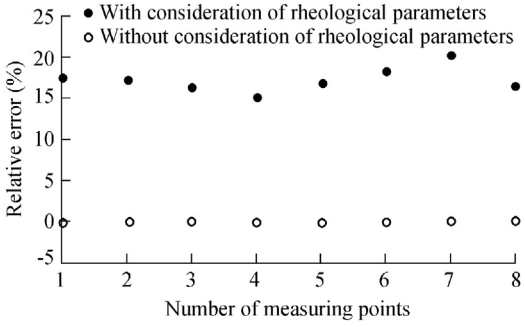

Fig. 5. Effect of rheological parameters on prediction accuracy of RSM.

$$\min E = \sqrt{\frac{1}{3}\sum_{q=1}^{3}\left[\frac{1}{T}\sum_{k=1}^{T}\left(S_{kq}(\boldsymbol{x}) - S'_{kq}\right)^2\right]} \tag{13}$$

where T is the total number of selected measuring points for back analysis, which equals 8; q is the characteristic moment number (1, 2, and 3 represent the completion period, impoundment period, and stable period, respectively); $S_{kq}(\boldsymbol{x})$ is the response surface function of measuring point k at characteristic moment q; and S'_{kq} is the measured value of measuring point k at characteristic moment q.

The response surface function of the measuring points was substituted into the objective function (Eq. (13)) to obtain the optimal parameters by solving the minimum value of the objective function using the improved GA in Matlab, as shown in Table 4.

The finite element parameter inversion calculation results and the measured data of the dam deformation have consistent development rules and values, as shown in Fig. 6. The results show that the inverted parameters in this study are reasonable and can reflect the actual deformation characteristics of the rockfills.

Table 4
Inversion results of EB model and creep model parameters of Shuibuya CFRD based on RSM.

Material	Creep model inverted parameter					EB model inverted parameter			
	α	b (10^5)	m_c	β (10^3)	d (10^3)	K	n	K_b	m
Primary rockfill	0.00722	11.8	1.360	7.679	2.511	881.133	0.280	480.090	0.080
Secondary rockfill	0.00722	11.8	1.360	7.679	2.511	682.780	0.201	320.296	0.041

The Shuibuya CFRD was analyzed using the inversion parameters with the finite element method. Figs. 7−9 show the settlement and horizontal displacement contour maps of the maximum section of the dam body at different moments. The calculation results show that the dam settlement increases strongly in the impoundment period and increases slightly in the stable period. The maximum settlement reached approximately 2.80 m in the stable period. After the impoundment, the overall displacement of the dam body, particularly the upstream part of the dam body, is in the downstream direction. The maximum horizontal displacement reaches approximately 50 cm downstream, which is noticeable. The distribution of the overall deformation of the dam body and its variation with time are consistent with the general rule.

In Figs. 7−9, the settlement of the dam increases substantially after the water storage. There is a slight increase of displacement from the impoundment period to the stable period. After the water storage, the entire dam moves downstream. Thus, the inverted parameters obtained in this paper

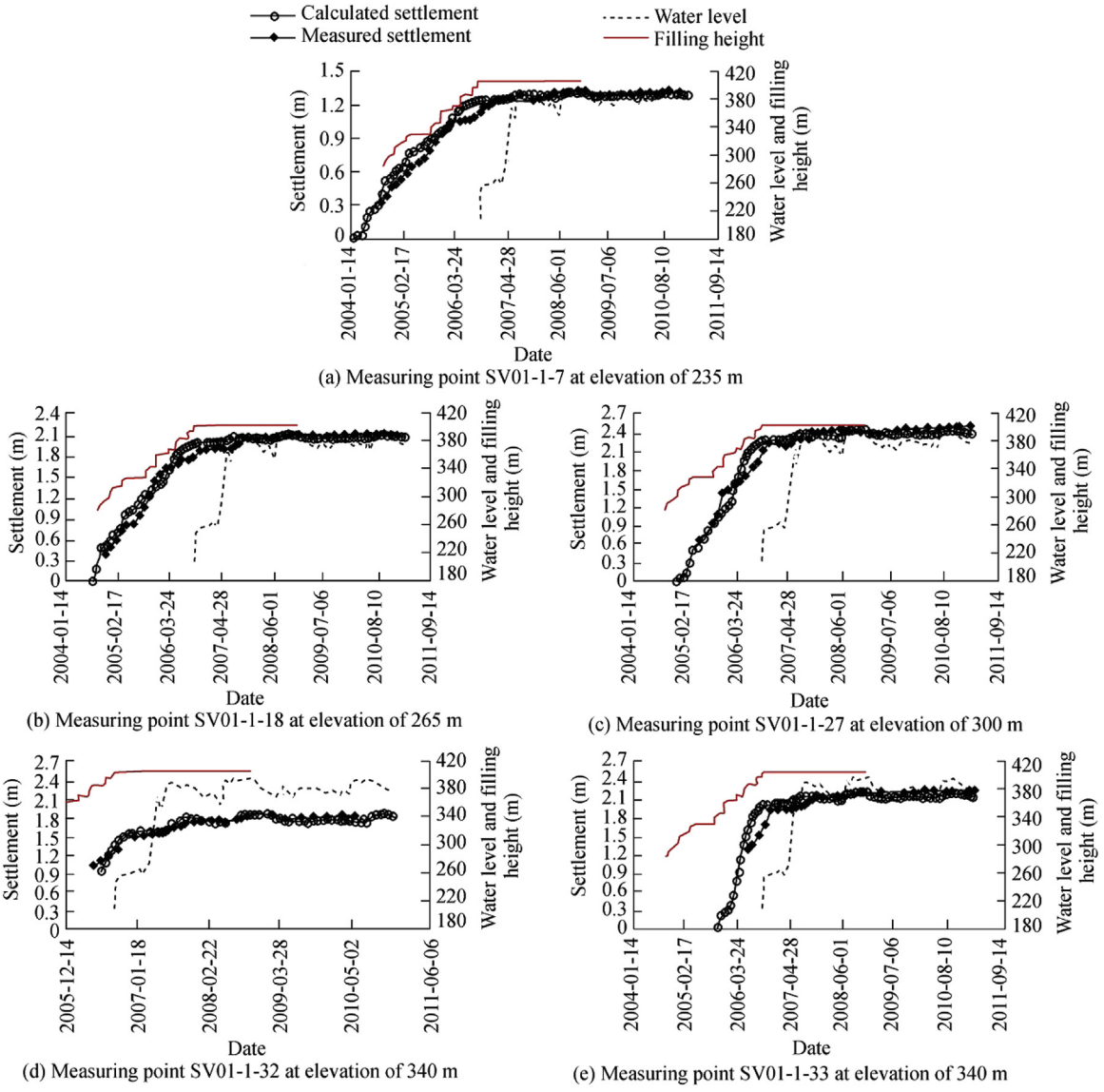

Fig. 6. Comparison between measured and calculated settlements at some measuring points in (0 + 212 m) section.

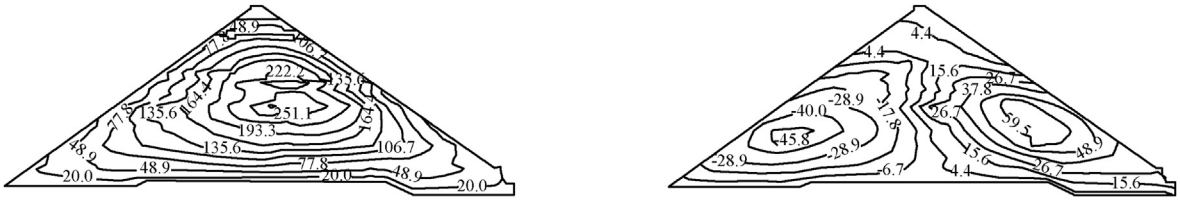

(a) Vertical displacement (positive: downward) (b) Displacement along river (positive: downstream)

Fig. 7. Predicted displacements at largest section of dam in completion period (units: cm).

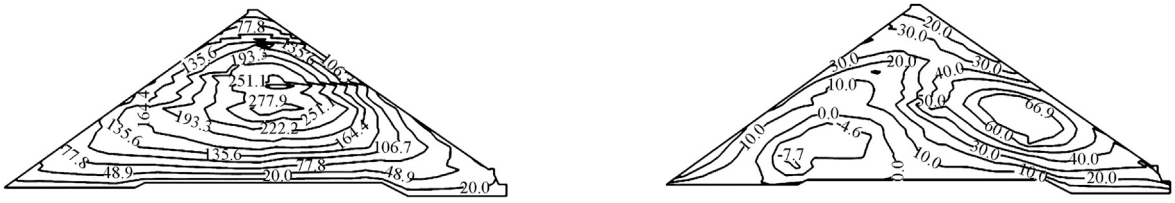

(a) Vertical displacement (positive: downward) (b) Displacement along river (positive: downstream)

Fig. 8. Predicted displacements at largest section of dam in impoundment period (units: cm).

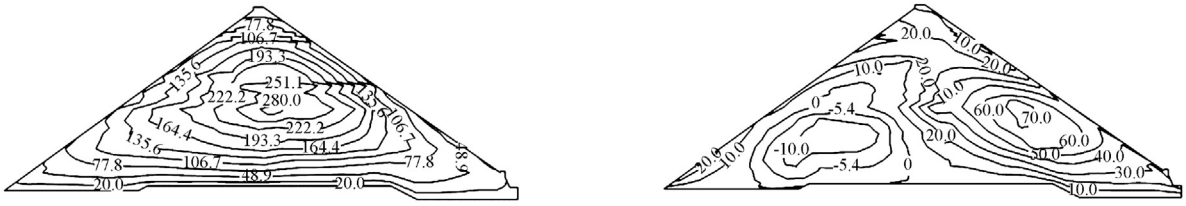

(a) Vertical displacement (positive: downward) (b) Displacement along river (positive: downstream)

Fig. 9. Predicted displacements at largest section of dam in stable period (units: cm).

reflect the true mechanical deformation characteristics of the dam material.

5. Conclusions

The RSM requires only 27 sets of training samples to invert both the Duncan EB and creep model parameters. It improves computational efficiency compared with ANNs, which requires 300 samples to invert only instantaneous deformation parameters. The Duncan EB model parameters K and K_b, obtained from back analysis, are smaller than those obtained from laboratory triaxial tests. The inverted creep model parameters indicate that the time-dependent deformation of prototype rockfill is larger and decays more slowly than the laboratory creep test results. The settlements calculated by finite element simulation with inverted parameters are closer to the measured dam deformation. The settlements develop quickly during the completion period and the impoundment period and increase slightly in the stable period, subject to rheologic deformation, which coincides with the general trend. The results demonstrate the accuracy and efficiency of the RSM for rockfill parameter back analysis.

References

Abusam, A., Keesman, K.J., Van, G.S., Spanjers, H., Meinema, K., 2001. Parameter estimation procedure for complex non-linear systems: Calibration of ASM No. 1 for N-removal in a full-scale oxidation ditch. Water Sci. Technol. 43(7), 357−365.

Cao, L., Zhan, Z.B., Han, Y., 2012. Deformation prediction and inversion of Shuibuya project based on artificial neural network and genetic algorithm. Appl. Mech. Mater. 170−173, 2115−2118. https://doi.org/10.4028/www.scientific.net/AMM.170-173.2115.

Chang, X., Yu, S., Ma, G., Zhou, W., 2011. Particle swarm optimization based on particle migration and its application to geotechnical engineering. Rock Soil Mech. 32(4), 1077−1082 (in Chinese). https://doi.org/10.16285/j.rsm.2011.04.041.

Dong, W.X., Yuan, H.N., Xu, W.J., Zhang, B.Y., Yu, Y.Z., 2012. Dynamic back-analysis of material parameters of Nuozhadu high earth-rock-fill dam. J. Hydroelectr. Eng. 31(5), 203−208 (in Chinese).

Dou, Y.F., Liu, F., Zhang, W.H., 2007. Research on comparative analysis of response surface methods. J. Eng. Des. 14(5), 359−363 (in Chinese). https://doi.org/10.3785/j.issn.1006-754X.2007.05.003.

Gui, J.S., Kang, H.G., 2005. Improved BP ANN response surface method for structural reliability analysis. Chin. J. Appl. Mech. 22(1), 127−130 (in Chinese). https://doi.org/10.3969/j.issn.1000-4939.2005.01.030.

Guo, Q.Q., Pei, L., Zhou, Z.J., Chen, J.K., Yao, F.H., 2016. Response surface and genetic method of deformation back analysis for high core rockfill dams. Comput. Geotech. 74, 132−140. https://doi.org/10.1016/j.compgeo.2016.01.001.

Hai, Y., Wang, R.J., 2005. Stress deformation and material sensitivity analysis of Gongboxia CFRD. Power System Clean Energy 21(2), 21−23, 27 (in Chinese). https://doi.org/10.3969/j.issn.1674-3814.2005.02.007.

He, J.T., Zhang, J., Huang, H.W., Zhang, Y.G., 2012. Back analysis of displacements of excavation based on multiple response surface method. Rock Soil Mech. 33(12), 3810−3817 (in Chinese). https://doi.org/10.16285/j.rsm.2012.12.027.

Hu, R., Chen, Y.F., Li, D.Q., Zhou, C.B., Tang, X.S., 2012. Reliability analysis of seepage stability of core-wall rockfill dam based on stochastic response surface method. Rock Soil Mech. 33(4), 1051−1060 (in Chinese). https://doi.org/10.16285/j.rsm.2012.04.036.

Ji, S.W., Zheng, M.S., Weng, Z., 2014. Analysis of stress and deformation of rockfill and concrete face for high concrete face rockfill dam. Appl. Mech. Mater. 638−640, 731−734. https://doi.org/10.4028/www.scientific.net/AMM.638-640.731.

Lei, G., Shen, Z.Z., Xu, L.Q., 2014. Long-term deformation analysis of the Jiudianxia concrete-faced rockfill dam. Arabian J. Sci. Eng. 39(3), 1589−1598. https://doi.org/10.1007/s13369-013-0788-6.

Li, D.Q., Zhou, C.B., Chen, Y.F., Jiang, Q.H., Rong, G., 2010. Reliability analysis of slope using stochastic response surface method and code implementation. Chin. J. Rock Mech. Eng. 29(8), 1513−1523 (in Chinese).

Li, S., Liu, X.Y., Chen, C.L., Li, Z.G., He, X., Zhou, Y.P., 2004. Inversion procedure for mechanical parameters of concrete dam with hybrid genetic algorithm. J. Dalian Univ. Technolgy 44(2), 195−199 (in Chinese).

Li, S.J., Zhang, J., Liang, J.Q., Sun, Z.X., 2014. Parameter inversion of nonlinear constitutive model of rockfill materials using observed deformations after dam construction. Rock Soil Mech. 35(s2), 61−67 (in Chinese). https://doi.org/10.16285/j.rsm.2014.s2.058.

Li, Y.L., Li, S.Y., Ding, Z.F., Tu, X., 2013. The sensitivity analysis of Duncan-Chang E-B model parameters based on the orthogonal test method. J. Hydraul. Eng. 44(7), 873−879 (in Chinese). https://doi.org/10.13243/j.cnki.slxb.2013.07.012.

Liu, Z.P., Chi, S.C., Ren, X.Y., 2014. Back analysis of dynamic parameters of dam materials based on earth-rockfill dam dynamic characteristics. Rock Soil Mech. 35(9), 2594−2601 (in Chinese). https://doi.org/10.16285/j.rsm.2014.09.027.

Ma, G., Chang, X.L., Zhou, W., Hua, J.J., 2012. Integrated inversion of instantaneous and rheological parameters and deformation prediction of high rockfill dam. Rock Soil Mech. 33(6), 1889−1895 (in Chinese). https://doi.org/10.16285/j.rsm.2012.06.036.

Saboya, F., Byrne, P.M., 1993. Parameters for stress and deformation analysis of rockfill dams. Can. Geotech. J. 30(4), 690−701. https://doi.org/10.1139/t93-058.

Shen, Z.J., Zhao, K.Z., 1998. The deformation of rockfill rheology feedback analysis. J. Hydraul. Eng. 29(6), 1−6 (in Chinese). https://doi.org/10.13243/j.cnki.slxb.1998.06.001.

Sheng, Q.Q., Wang, X.R., Xie, Z.Q., Zheng, Z.Q., 2012. The parameter inversion and stress simulation analysis for high RCC gravity dam in construction. Appl. Mech. Mater. 182−183, 1600−1604. https://doi.org/10.4028/www.scientific.net/AMM.182-183.1600.

Su, C., Li, P.F., Han, D.J., 2009. Neumann-expansion response surface method for calculating structure reliability. J. South China Univ. Technol. 37(9), 12−13 (in Chinese). https://doi.org/10.3321/j.issn:1000-565X.2009.09.003.

Sun, P.M., Bao, T.F., Gu, C.S., Jiang, M., Wang, T., Shi, Z.W., 2016. Parameter sensitivity and inversion analysis of a concrete faced rock-fill dam based on HS-BPNN algorithm. Sci. China Technol. Sci. 59(9), 1442−1451. https://doi.org/10.1007/s11431-016-0213-y.

Tian, Z.R., Li, S.J., Shen, Y., 2014. Inversion of rock mass mechanical parameter in underground powerhouse of Baishan pumped storage station. Rock Soil Mech. 35(s2), 508−513 (in Chinese). https://doi.org/10.16285/j.rsm.2014.s2.062.

Wang, G.Q., Yu, T., Li, Y.H., Li, G.Y., 2014a. Creep deformation of 300 m-high earth core rockfill dam. Chin. J. Geotech. Eng. 36(1), 140−145 (in Chinese). https://doi.org/10.11779/CJGE201401013.

Wang, X., Kang, F., Li, J.J., 2014b. Back analysis of earthquake-induced permanent deformation parameters of earth-rock dams. Rock Soil Mech. 35(1), 279−286 (in Chinese). https://doi.org/10.16285/j.rsm.2014.01.032.

Wang, Y.F., Wang, C.G., 2005. The application of response surface methodology. J. Cent. Univ. Natl. 14(3), 236−240 (in Chinese). https://doi.org/10.3969/j.issn.1005-8036.2005.03.008.

Wu, Y.K., Yuan, H.N., Zhang, B.Y., Zhang, Z.L., Yu, Y.Z., 2014. Displacement-based back-analysis of the model parameters of the Nuozhadu high earth-rockfill dam. Sci. World J. 2014, 1−10. https://doi.org/10.1155/2014/292450.

Yang, C.Y., Zhang, M., Bai, X.L., 2001. Multiple response surface method in analysis of structural reliability. J. North. Jiaot. Univ. 25(1), 1−4 (in Chinese). https://doi.org/10.3969/j.issn.1673-0291.2001.01.001.

Yang, H., Xie, S.Y., Secq, J., Shao, J.F., 2017. Experimental study and modeling of hydromechanical behavior of concrete fracture. Water Sci. Eng. 10(2), 97−106. https://doi.org/10.1016/j.wse.2017.06.002.

Yang, L.F., Li, Z.Y., Yang, X.F., 2012. Vectorial cooperative response surface method for structural reliability. China Civ. Eng. J. 45(7), 105−110 (in Chinese). https://doi.org/10.15951/j.tmgcxb.2012.07.024.

Yeh, W.W.G., 1986. Review of parameter identification procedures in groundwater hydrology: The inverse problem. Water Resour. Res. 22(2), 95−108. https://doi.org/10.1029/WR022i002p00095.

Zhang, L., Zhang, G., Wang, F.Q., Zhang, J.M., 2011. Rheological deformation back-analysis for Gongboxia concrete faced rockfill dam. Rock Soil Mech. 32(s2), 521−525 (in Chinese). https://doi.org/10.16285/j.rsm.2011.s2.076.

Zhang, S.R., He, H., 2005. Application of improved genetic algorithm to back analyzing parameters of rockfill. Rock Soil Mech. 26(2), 182−186 (in Chinese). https://doi.org/10.16285/j.rsm.2005.02.003.

Zhang, Z.L., Jia, Y.A., Zhang, B.Y., 2008. Comparison and verification of constitutive models for rockfill materials under complex stress path. Rock Soil Mech. 29(5), 1147−1151 (in Chinese). https://doi.org/10.16285/j.rsm.2008.05.028.

Zheng, D., Cheng, L., Bao, T., Lü, B., 2013. Integrated parameter inversion analysis method of a CFRD based on multi-output support vector machines and the clonal selection algorithm. Comput. Geotech. 47, 68−77. https://doi.org/10.1016/j.compgeo.2012.07.006.

Zhou, W., Xu, G., Chang, X.L., Hu, Y., 2007. Intelligent back analysis on parameters of creep constitutive model. J. Hydraul. Eng. 38(4), 389−394 (in Chinese). https://doi.org/10.13243/j.cnki.slxb.2007.04.002.

Zhou, W., Chang, X.L., Zhou, C.B., Liu, X.H., 2010. Creep analysis of high concrete-faced rockfill dam. Int. J. Numer. Methods Biomed. Eng. 26(11), 1477−1492. https://doi.org/10.1002/cnm.1230.

Zhou, W., Hua, J.J., Chang, X.L., Zhou, C.B., 2011a. Settlement analysis of the Shuibuya concrete-face rockfill dam. Comput. Geotech. 38(2), 269−280. https://doi.org/10.1016/j.compgeo.2010.10.004.

Zhou, W., Ma, G., Chao, H., 2011b. Long-term deformation control theory of high concrete face rockfill dam and application. In: Proceedings of Asia-Pacific Power & Energy Engineering Conference. IEEE Computer Society. https://doi.org/10.1109/APPEEC.2011.5748895.

Zhou, W., Li, S.L., Zhou, Z.W., Chang, X.L., 2016a. Remote sensing of deformation of a high concrete-faced rockfill dam using insar: A study of the Shuibuya dam, China. Remote Sens. 8(3), 255. https://doi.org/10.3390/rs8030255.

Zhou, W., Li, S.L., Zhou, Z.W., Chang, X.L., 2016b. Insar observation and numerical modeling of the earth-dam displacement of Shuibuya Dam (China). Remote Sens. 8(10), 877. https://doi.org/10.3390/rs8100877.

Zhou, W., Li, S.L., Ma, G., Chang, X.L., Ma, X.L., Zhang, C., 2016c. Parameters inversion of high central core rockfill dams based on a novel genetic algorithm. Sci. China Technol. Sci. 59(5), 783−794. https://doi.org/10.1007/s11431-016-6017-2.

Zhou, X., Ma, G., Zhang, Y., 2018. Grain size and time effect on the deformation of rockfill dams: A case study on the Shuibuya CFRD. Geotechnique 69(7), 606−619. https://doi.org/10.1680/jgeot.17.P.299.

Zhu, S., Yang, G., Zhou, J.P., Song, Y.G., 2010. Back analysis on static and dynamic characteristics of Zipingpu CFRD under "5·12" Wenchuan earthquake. J. Sichuan Univ. (Eng. Sci. Ed.) 42(5), 113−119 (in Chinese). https://doi.org/10.15961/j.jsuese.2010.05.017.